Bond Performance of the Slurry Infiltrated Fiber Concrete Overlay on Normal Strength Concrete Substrate

Mohammed F. Ojaimi
Department of Civil Engineering, College of Engineering, University of Basrah, Basra, Iraq
mohammed.ojaimi@uobasrah.edu.iq (corresponding author)

David A.M. Jawad
Department of Civil Engineering, College of Engineering, University of Basrah, Basra, Iraq
david.jawad@uobasrah.edu.iq

Abdullah A. Al-Hussein
Department of Civil Engineering, College of Engineering, University of Basrah, Basra, Iraq
abdullah.amir@uobasrah.edu.iq

Received: 26 June 2025 | Revised: 23 July 2025 | Accepted: 27 July 2025

 DOI: https://doi.org/10.48084/etasr.12968

ABSTRACT

Many concrete structures require strengthening or repair and a significant method of strengthening the Reinforced Concrete (RC) members is to add a concrete jacket. A type of concrete known as Slurry-Infiltrated Fiber Concrete (SIFCON) has come into use. SIFCON is a unique form of Fiber-Reinforced Concrete (FRC) known for its superior mechanical properties. The effectiveness of upgrading the RC members through jacketing depends on several factors, the most important of which is the bond performance between the substrate and overlay layers. This study examined how various factors influence the bonding performance between the SIFCON overlay and the Normal Strength Concrete (NSC) substrate. The research investigated the effects of surface preparation methods, types of bonding agents, and steel fiber geometry. Three tests were conducted to evaluate the bond strength: the Slant Shear Test (SST), Tensile Bond Test (TBT), and Flexural Bond Test (FBT). The surface preparation methods ranked from best to worst as follows: Grinding (G), Sandblasting (S), and Diamond Cutting (DC). The increase in the bond strength depended on the type of bonding agent and the surface preparation method. When the failure mode changed from Bond Interface (BI) to both BI and Weaker Concrete (BI-WC) or from BI-WC to WC, the increase was noticeable. If the failure mode shifted directly from BI to WC, the growth was significant. However, if the failure mode remained the same, the increase was minimal.

Keywords-bond; interface; SIFCON; overlay; Slant Shear Test (SST); jacketing; Tensile Bond Test (TBT); surface preparation; bond agent

I. INTRODUCTION

For various reasons, including design errors, construction failures, or exposure to loads that exceed their design capacity, many concrete structures require strengthening or repair [1, 2]. One significant approach is to expand the structural members with an externally bonded concrete jacket. Various types of concrete have been developed, with SIFCON being the best choice. SIFCON is a unique form of FRC, distinguished for its superior mechanical properties [3, 4]. SIFCON differs from FRC in three key aspects: fiber content, preparation method, and mixture components, with the latter having a fiber content that does not exceed 3%. Using a fiber volume fraction greater than this ratio hinders the proper mixing and leads to a non-homogeneous mixture [5, 6]. In contrast, SIFCON allows for fiber content levels of up to 30%, depending on the fiber's shape and dimensions [3, 7]. Typically, the fiber content ranges from 4% to 10% for common fiber dimensions [8]. SIFCON's ability to achieve high fiber content stems from its manufacturing process: first, the mold is filled with fiber; then, the slurry is poured over the fiber [9]. SIFCON's high fiber content provides superior mechanical properties, making it a suitable option for strengthening and repairing the concrete structural members. However, SIFCON is more expensive than other common types of concrete due to its high cement content and the large number of fibers required during production. Researchers have focused on developing SIFCON to enhance its sustainability and mechanical properties and reduce the production costs by using recycled or by-product materials.

Authors in [10-12] developed an alkali-activated slag SIFCON using recycled glass, and waste steel fibers from scrap tires and found that producing SIFCON with recycled or by-product materials can achieve comparable mechanical properties to those of ordinary SIFCON while offering better cost and sustainability results. The effectiveness of upgrading the RC members through jacketing depends on several factors, with one of the most important being the bond performance between the substrate and overlay layers [13, 14]. Various tests are available to assess the bonding performance between old and new concrete. Previous researchers have reported that the following factors significantly affect the bond strength: surface preparation method, binder type, mechanical properties of the surface and overlay concrete, mechanical bonding, and the use of dowels in the bond system [15-17]. Authors in [18] examined the bond performance of various concrete repair material overlays on NSC substrates. The researchers conducted an SST to investigate the effects of various factors on the bond strength between the old and new concrete. These factors included the age difference between the layers of concrete, the method used to prepare the substrate surface, the type of bonding agent, and the type of new concrete. The study concluded that an increased age difference between the old and new layers significantly decreases the bonding resistance. Compared to models with a three-day age difference, the bonding resistance decreased by 16.6%, 25.4%, and 28% when the age difference was 7, 28, and 365 days, respectively. Authors in [19] studied the bond strength of fly ash-based polymer overlays on ordinary Portland cement concrete substrates. Their research involved verifying the bond performance between new and old layers under various substrate surface conditions, with a focus on the surface roughness and humidity, to simulate the acidic environment of sewer pipes. Cylinders measuring 50 mm in diameter and 100 mm in length, cut at a 45° angle, were used in the SST to evaluate the bond strength between the substrate and the overlay. The study compared the bonding performance of various geopolymer mortars with that of ordinary Portland cement mortar. The researchers concluded that the low calcium fly ash-based polymer had the best bond strength among the examined repair materials under all studied conditions. Authors in [20] studied the factors influencing the bond strength between the NSC substrates and Self-Compacting Concrete (SCC) overlays. The study examined how the compressive strength of the substrate and overlay layers, the type of bonding agent, substrate roughness, latex incorporation in the SCC mixture, and polypropylene addition to the SCC affected the bond strength. Additionally, the authors investigated the appropriate shape and dimensions of the SST specimen. Cylinders and prisms were used, concluding that a cylinder with a diameter of 150 mm and a height of 300 mm yielded the lowest coefficient of variation compared to the other specimen geometries studied. Furthermore, prism slant shear specimens yield more reliable bond strength values than cylinders. Authors in [21] proposed a Modified SST (M-SST) model based on the commonly used SST model. They stated that, although the SST test is widely used, it often fails to accurately evaluate the actual interfacial bond strength, providing only a lower estimate of strength at the contact surface. This occurs because the WC of the substrate or overlay layer often fails before the interfacial bond, resulting in cohesive failure. Therefore, the M-SST includes a 6 mm steel reinforcement in both the substrate and overlay layers to ensure the adhesive interface debonding failure and prevent the cohesive failure. Additionally, the researchers conducted a numerical study concluding that the steel reinforcement does not alter the stresses at the interface.

II. RESEARCH SIGNIFICANCE

The existing body of research has not yet addressed the factors influencing the bonding performance between NSC and SIFCON. SIFCON is a material that is abundant in cement, silica fume, fly ash, and fibers, having a direct impact on the bond strength. Therefore, the objective of this study was to examine the bond performance of the SIFCON overlay on the NSC substrate.

III. EXPERIMENTAL PROGRAM

The present study sets a series of bonding techniques for connecting the conventional concrete substrate to the novel overlay of SIFCON. A thorough examination into the factors that influence the bond strength is important, including the bonding agent material, the method of preparing the surface of the old concrete substrate, and the type of steel fiber. A series of experimental tests were conducted to ascertain the most effective technique for achieving a robust bond, at the Civil Engineering Department laboratory at Basrah University.

A. Materials

Ordinary Portland cement type I (Aljesser), was used in the construction of the concrete elements, meeting the requirements of ASTM C150 [22]. The present study applied densified micro silica that complies with the standard specifications of ASTM C1240 [23] from the CONMIX-UAE company (MegaAdd MS(D)). The bulk density and specific gravity of the silica fume were determined to be 630 kg/m^3 and 2.22 kg/m^3, respectively. Table I presents the chemical components of the cement and silica fume, while Table II presents the physical properties of the cement.

TABLE I. CHEMICAL PROPERTIES OF THE CEMENT AND THE SILICA FUME

Chemical composition	**Chemical composition (%)**	
	Cement	Silica fume
CaO	60.8	0.45
SiO2	22.1	92.0
Al_2O_3	6.2	0.90
Fe_2O_3	3.0	1.95
MgO	2.6	0.98
SO3	2.2	0.31
L.O.I.	1.6	1.8
Moisture content (H_2O)	-----	0.93

TABLE II. PHYSICAL PROPERTIES OF THE CEMENT

Physical properties	**Test result**
Fineness, specific surface, air permeability test	339 m^2/kg
Compressive strength	
3 days	18.3 MPa
7 days	25.4 MPa
Time of setting; Vicat test	115 min
Specific gravity	3.15

Two grades of natural sand were used in the study: one for NSC, which meets ASTM C33 [24] specifications, and the other for SIFCON, with a maximum grain size of 1.18 mm. Figure 1 presents the grading curves of the sand in NSC. Crushed gravel, with a nominal size ranging from 19 mm to 4 mm, satisfied the standard specifications of ASTM C33 [24] and was used to produce NSC, while Figure 2 shows the grading curves of the gravel in NSC. The experimental work used the commercial product MasterGlenium 200 (from BASF), a third-generation superplasticizer and High-range Water Reducer (HRWR) with a chemical base of polycarboxylic ether. The material exhibits compatibility with silica fume and fly ash, thereby meeting the standard specifications outlined in ASTM C494 [25] type D&G. As depicted in Figure 3, this study used five distinct steel fiber geometries: three had a length that exceeded 10 cm, while two were classified as micro steel fibers, with a diameter of less than 1 mm. The aspect ratio of the steel fibers used was 60 and had 30 mm length, 0.5 mm diameter, and possessed a tensile strength of 1100 MPa. The distinguishing factor among the fibers was their shape: Hook-ended (H), Waved (W), and Straight (S). The properties of the two micro steel fibers were: 13 mm in length, 0.22 mm in diameter, and 2850 MPa in tensile strength. One specimen was classified as Micro-Straight (MS), while the other was designated as Micro-Hook-ended (MH). The present study used two types of bonding agent materials to connect the hardened substrate with the fresh SIFCON. The initial substance was identified as an epoxy resin, while the secondary substance was determined to be a synthetic rubber emulsion, also known as latex (Sikadur-32 LP and SikaLatex-IQ).

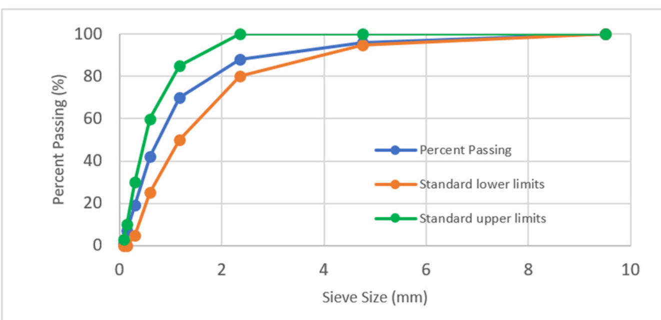

Fig. 1. Grading curves of the sand in NSC.

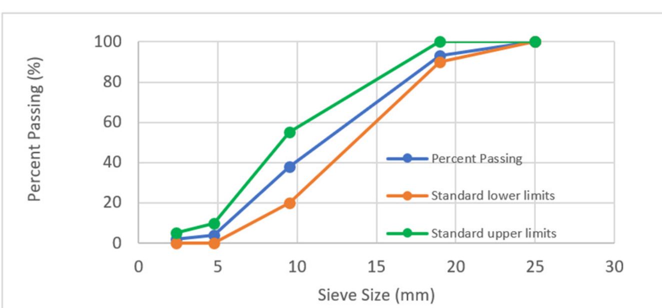

Fig. 2. Grading curves of the gravel in NSC.

B. *Mixtures of the Substrate and Overlay SIFCON*

The mixture proportion employed in this study to prepare NSC by weight was 1:1.8:2.7 (cement: sand: gravel). The water-to-binder (w/b) and superplasticizer-to-binder (sp/b) ratios were determined to be 0.42 and 0.0075, respectively. The slump value of the NSC was 215 mm and an equal amount of sand and binder was used to produce the slurry, with 10% of the cement replaced by silica fume. The w/b and sp/b ratios were determined to be 0.3 and 0.02, respectively, as shown in Table III.

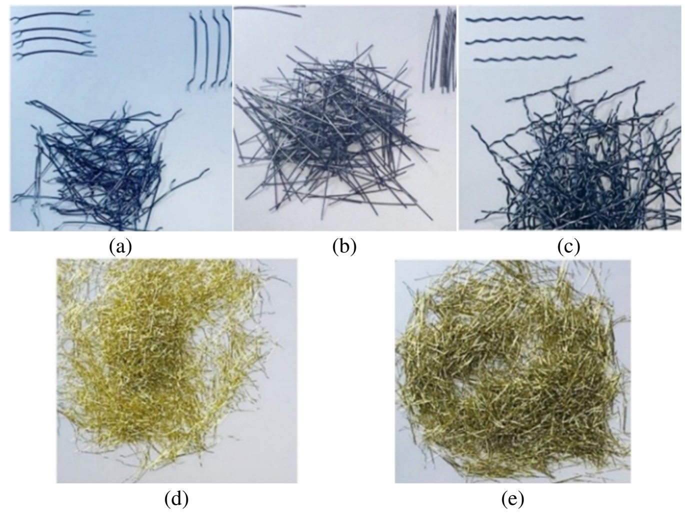

Fig. 3. Steel fibers: (a) H, (b) S, (c) W, (d) MH, (e) MS.

TABLE III. MIX PROPORTIONS FOR RESPECTIVE 1M^3 OF NORMAL-STRENGTH CONCRETE AND SLURRY

Material	NSC	Slurry
Cement (kg/m^3)	400.0	882.0
Silica fume (kg/m^3)	-	98.0
Sand (kg/m^3)	720.0	946.0
Gravel (kg/m^3)	1080.0	-
Tap water (kg/m^3)	168.0	294.0
Superplasticizer (kg/m^3)	3.0	19.6

C. *SIFCON Production*

A novel strategy was used to mix the slurry components, ensuring proper mixing and homogeneity. Initially, the cement was amalgamated with silica fume for a duration of 1 min, using a high-speed electric drill. Subsequently, sand was added to the mixture and blended with the same mixer for an additional min. A total of 33.33% of the water was combined with HRWR for a duration of half a min. Subsequently, the dry mix was transferred to a standard-speed drum mixer, wherein the liquid obtained from the amalgamation of water and HRWR was integrated. The materials were then subjected to a 1 min mixing period and the remaining water was then gradually added to the mixture, with the process of mixing continuing for a period of 5 min, as portrayed in Figure 4. In this research, the molds were filled in layers, with each layer measuring no more than 25 mm in thickness. The slurry was poured into the mold, and the steel fibers were dispersed in a random configuration and subsequently compacted using a steel rod. This process was repeated until the mold was filled. The maximum available fiber volume fraction was taken into consideration. The fiber content of the steel fiber in the SIFCON is significantly dependent on the geometry of the steel fiber, with H, W, S, MH, and MS fibers being 7%, 6.8%, 7.5%, 6%, and 7.8%, respectively.

Fig. 4. Slurry mixing process.

D. The Curing Regime and Tests of the NSC and SIFCON in Fresh and Hardened States

Tests for compressive strength, flexural strength, and splitting tensile strength were conducted at 28 days to assess the mechanical properties of NSC and SIFCON. Three individual samples were used for each test, and the demolding of them occurred 24 h after casting. The NSC samples were stored in a container filled with tap water at room temperature until the test date, while the SIFCON samples were exposed to dry air for the same duration. The SIFCON samples were cured in dry air conditions to prevent water from adversely affecting the chemical reactions of the bonding agents used to join the two types of concrete. Cylinders with a diameter of 75 mm and a length of 150 mm were used to assess the compressive strength and tensile strength of the NSC and SIFCON. The flexural strength of the beams was determined through third-point loading, with the beams measuring 100 mm x 100 mm x 400 mm. The tensile and flexural strength tests were conducted in accordance with the standards of ASTM C496 [26] and ASTM C78 [27], respectively. Achieving adequate flowability in the slurry is important to ensure a complete infiltration between the fibers and to prevent blockage, honeycombing, and bleeding. To assess the slurry's workability, a series of tests were conducted, including mini-slump flow and V-funnel tests, in accordance with the standards of ASTM C1437 [28] and EFNARC [29]. Authors in [30] determined that the acceptable range for the spread diameter in the mini-slump flow test is from 350 mm to 380 mm, and that the acceptable flow time in the V-funnel test is from 6 to 11 s.

E. Tests Assessing the Bond Performance of the NSC Substrate and SIFCON Overlay

To ascertain the bond performance between the existing RC beams and the newly installed SIFCON jackets, three tests were conducted: the SST, TBT, and FBT. According to ACI 546.3R-14 [31], the performance of the slant shear, splitting tensile strength, and flexural strength tests is dependent upon the preparation of the interfacial surface through grinding, sandblasting, or diamond cutting. During the examination of the samples, if failure occurs away from the bond line between the surfaces of the old and new concrete, it indicates that the bond strength is greater than the force that caused the failure of the sample. In the event of failure at the bond line between the old and new concrete, the bond strength measured from the test represents the actual strength between the two examined surfaces. Subsequent to the casting process, all samples representing the substrate layer were demolded 24 h post-casting and submerged in a container filled with normal temperature tap water for a period of 28 days. The bonding process of the SIFCON overlay was initiated and the samples were subjected to a curing process in dry air at room temperature for a period of 28 days.

1) Slant Shear Test

The SST is a method of measuring the sliding resistance between a new concrete layer and an existing normal concrete surface. The test is performed by inclining the surface at a 30° angle from the vertical cylinder axis. The interface line is subject to a combination of compressive and tensile stresses, in accordance with the standard specification ASTM C882 [32]. Initially, cylinders with a diameter of 75 mm and a length of 150 mm were cast using normal-strength concrete to prepare the substrate of the SST samples. Subsequent to the culmination of the 28-day curing period, the cylinder was sectioned using an electric concrete cutting machine at a 30° incline, thereby adhering to the recommended geometry outlined in ASTM C882 [32]. The concrete substrate was prepared through S, G, or a combination of both G and DC. Subsequently, the bonding agent was applied to the prepared surface, then the halved cylinder was placed in a new cylindrical mold, and the SIFCON was poured to fill the mold and create a composite cylinder of NC and SIFCON. Following a 28-day curing period in dry air at room temperature, the specimen was subjected to compression until failure. The bond strength is calculated by dividing the ultimate failure load by the elliptical area of the bonding surface. As shown in Figure 5, the test setup for the SST is composed of several components.

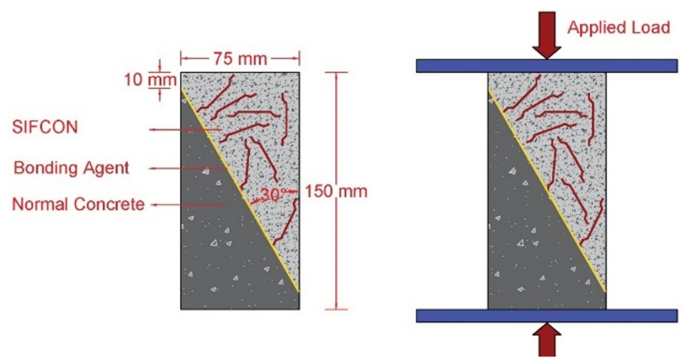

Fig. 5. SST setup.

The SST is a widely used method for evaluating the bond strength, proposed in [33]. To assess the bond strength of epoxy-based resins, a cylinder with a diameter of 150 mm and a height of 300 mm was used. Although the standard specification ASTM C882 [32] specifies a cut angle of 30° from the vertical axis for the SST, some researchers have reported that this angle is incompatible for all surface roughness conditions [34, 35]. Authors in [34] observed that the angle exhibits a preference for less than 30° when dealing with non-smooth substrate surfaces. The use of a 45° bond angle in the SST is optimal for the examination of the bond performance between the alkali-activated material overlay and the concrete substrate. It has been indicated that the cylinder dimensions outlined in the ASTM C882 [32] are suboptimal for the SST, resulting in elevated coefficients of variation for the obtained results. Alternative cylinder dimensions have been proposed and it has been concluded that these provide more stable results. It has been posited that the usage of a square cross-section prism is preferable to other options, as proposed by the BS EN 12615:1999 standard [20, 21].

2) Tensile Bond Strength Test (TBT)

The bonding tensile strength was evaluated through a splitting tensile test, which was performed in accordance with the standards outlined in ASTM C496 [26]. In this experiment, a compression load is applied along the longitudinal direction of the unconfined cylinder to divide the cylinder along its axis. The same procedure was used for the slant shear sample preparation to ensure the composite cylinder's readiness for the splitting tensile test. The only difference is that the cylinder was halved vertically in the splitting tensile sample, as shown in Figure 6.

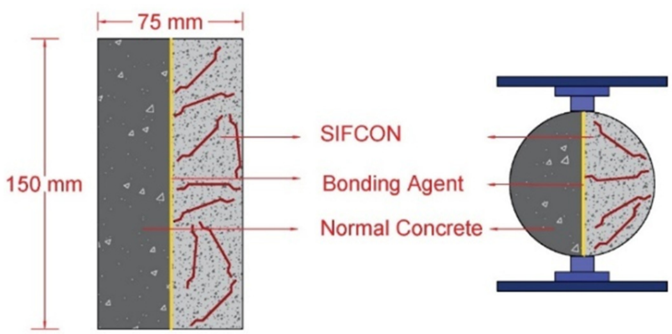

Fig. 6. Tensile bond strength test setup.

3) Flexural Bond Strength (FBS) Test

The FBS was assessed by initially casting beams measuring 100 mm × 100 mm × 400 mm using normal-strength concrete. After a period of 28 days, the beams were reduced by half at their mid-span, as shown in Figure 7. The substrate surface was prepared, and the bonding agent was applied and the remaining half was cast using SIFCON. The beams were subjected to bending tests in accordance with the standards outlined in ASTM C78 [27]. A two-point loading test was conducted with the maximum tensile stress occurring in the middle third of the beam, whereas in the one-point loading test, it occurs at a single cross-section at the mid-span. The schematic of the composed flexural test sample and its test setup is presented in Figure 8.

F. Substrate Surface Preparation and Details of the Used Bonding Systems

The present study examined three methods for preparing substrate surfaces: G, DC, and S. The effectiveness of two bonding agents was evaluated: the first component is epoxy resin (Sikadur-32 LP), and the second component is synthetic rubber emulsion latex (SikaLatex-IQ). The three methodologies for the surface preparation were evaluated, each with and without bonding agents. The arithmetic mean of the three tested samples was recorded to assess and compare the bonding techniques employed. Figure 9 exhibits how the test samples were subjected to slant shear, splitting tensile strength, and flexural strength tests following the surface preparation, and Figure 10 presents the terminology employed to describe a specimen that was tested.

Fig. 7. Steps for preparing the FBS test sample.

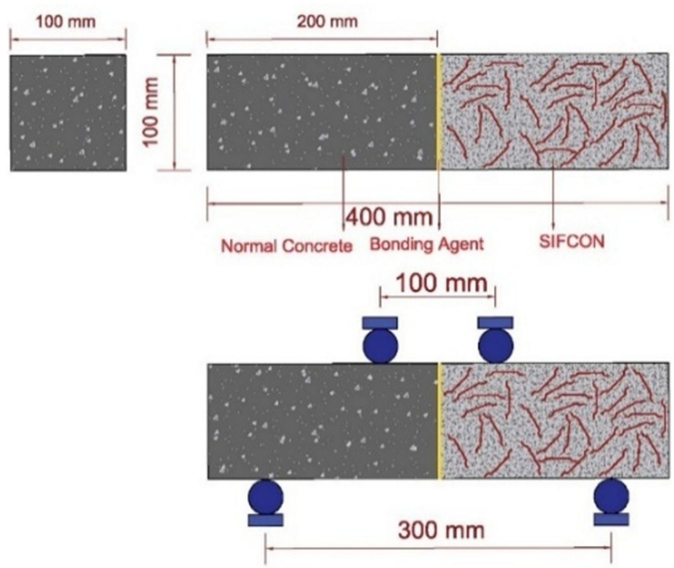

Fig. 8. FBS test setup.

IV. RESULTS AND DISCUSSION

The present study used NSC as the substrate and SIFCON as the overlay. The production of SIFCON involved the usage of five distinct geometries of steel fiber. Table IV presents the mechanical properties of the hardened NSC substrate and the SIFCON overlay for each geometry of steel fiber. The V-funnel time and mini-slump flow of the slurry used in the production of SIFCON were 10.1 s and 360 mm, respectively. Table V and Figure 11, display the mean values and standard deviations for the slant shear, flexural bond strength, and splitting tensile bond strength tests. The slant shear bond strength (σ_o) is calculated using (1) and reflects the vertical stress applied at the interfacial bond surface of the SST sample, leading to shear failure along the inclined bond plane. The slant shear strength (τ_n), which represents the shear stress imposed parallel to the sliding surface, is derived from [19, 36, 37]:

$$\sigma_o = \frac{P}{A_n} \tag{1}$$

$$\tau_n = \frac{P}{A_n} \sin\theta \, \cos\theta \tag{2}$$

where P and A_n are the failure load and the area of the inclined plane in the SST samples.

(a) (b) (c)

Fig. 9. The slant shear, splitting tensile strength, and the flexural strength test samples after surface preparation: (a) G, (b) G and DC, (c) sand blasting.

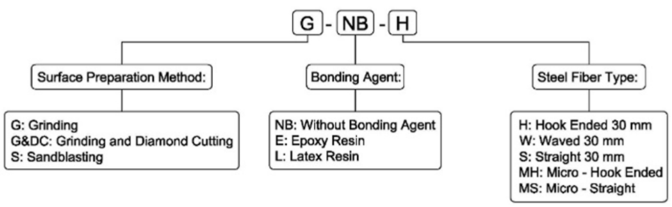

Fig. 10. The terminology used to describe one specimen.

TABLE IV. MECHANICAL PROPERTIES OF THE NSC AND SIFCON WITH DIFFERENT STEEL FIBERS

Type of concrete	Compressive strength (MPa)	Modulus of rupture (MPa)	Tensile strength (MPa)
NSC	34.0	3.9	2.3
SIFCON with (H) fiber	69.6	35.2	18.8
SIFCON with (W) fiber	56.2	28.1	14.6
SIFCON with (ST) fiber	65.4	26.4	13.5
SIFCON with (MH) fiber	49.8	22.1	10.6
SIFCON with (MS) fiber	48.5	20.7	9.5

TABLE V. THE MEASURED BOND STRENGTH ACCORDING TO THE SST, FBT, AND TBT (AV. ± ST. DEV.)

Specimen designation	Flexure bond strength (MPa)	Tensile bond strength (MPa)	Slant shear bond strength (σ_o) (MPa)	Slant shear strength (τ_n) (MPa)
G-NB-H	2.45 (± 0.9)	1.40 (± 1.4)	7.82 (± 2.2)	3.39 (± 2.2)
G-E-H	4.12 (± 0.8)	2.56 (± 1.2)	16.32 (± 2.3)	7.07 (± 2.3)
G-L-H	2.77 (± 1.1)	1.65 (± 1.1)	9.18 (± 1.7)	3.98 (± 1.7)
DC-NB-H	3.71 (± 1.0)	2.20 (± 0.9)	12.92 (± 2.5)	5.6 (± 2.5)
DC-E-H	4.30 (± 0.8)	2.71 (± 1.6)	18.70 (± 2.1)	8.10 (± 2.1)
DC-L-H	3.84 (± 1.2)	2.34 (± 1.4)	16.15 (± 1.8)	6.99 (± 1.8)
S-NB-H	3.65 (± 0.7)	2.08 (± 1.3)	12.24 (± 2.7)	5.30 (± 2.7)
S-E-H	4.19 (± 1.1)	2.60 (± 0.8)	17.00 (± 2.3)	5.89 (± 2.3)
S-L-H	3.72 (± 0.8)	2.23 (± 1.5)	13.60 (± 2.5)	7.36 (± 2.5)
DC-E-W	3.91 (± 0.7)	2.31 (± 1.4)	16.66 (± 1.5)	7.22 (± 1.5)
DC-E-S	3.96 (± 1.1)	2.32 (± 1.3)	17.34 (± 1.8)	7.51 (± 1.8)
DC-E-MH	4.01 (± 1.4)	2.41 (± 1.7)	15.98 (± 1.7)	6.92 (± 1.7)
DC-E-MS	4.07 (± 0.8)	2.46 (± 1.6)	15.30 (± 2.0)	6.63 (± 2.0)

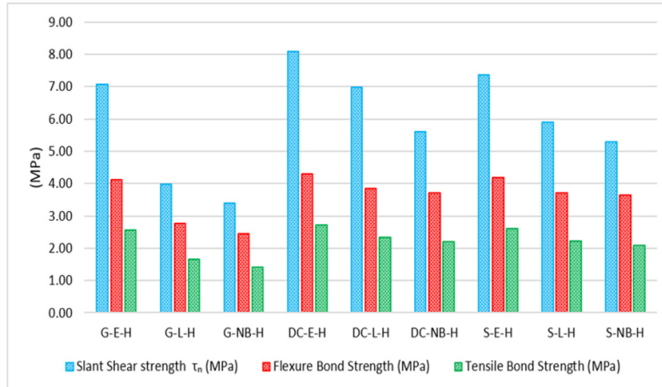

Fig. 11. The measured bond strength according to the SST, FBT, and TBT for the samples cast with SIFCON overlay produced by a 30 mm H steel fiber.

In this study, A is 8835 mm², a calculation determined by the specific cylinder dimensions and bond angle. Angle θ is defined as the inclination of the inclined interface plane, measured from the vertical axis. The preliminary findings from the testing process indicate that the failure modes observed in the SST and FBT can be classified into three distinct categories: WC, BI, and WC-BI. The identified modes of failure correspond to WC, BI, and the combination of WC and BI, respectively. Figures 12 and 13 provide examples of SST and FBS test failures in the WC, BI, and WC-BI modes. As presented in Figures 12 (a) and 13 (a), the failure was observed in the substrate concrete, with no visible cracks detected in the bond surface or the SIFCON layer. As shown in Figures 12 (b) and 13 (b), the failure occurred exclusively on the bond surface, with no evidence of cracking in the substrate or overlay layers. Figures 12 (c) and 13 (c) present cases in which failure occurred in both the bond surface and the substrate concrete. The failure mechanism in the splitting TBT differs from those of the previous two tests. Although the three failure modes were not evident during visual inspection, the observed failure mode in all tested specimens indicates that BI failure has occurred.

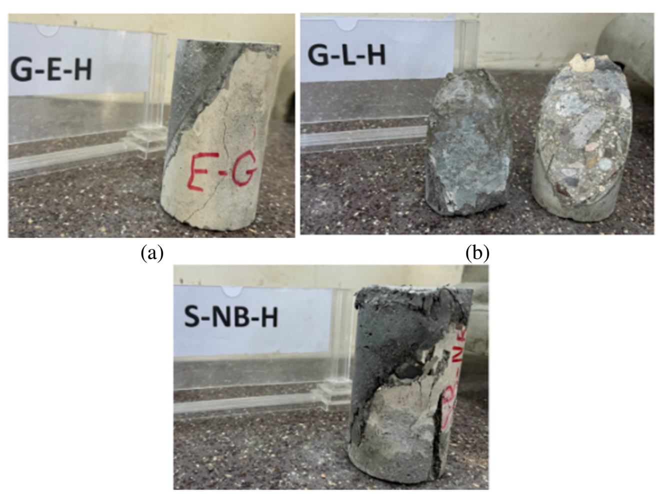

(a) (b)

(c)

Fig. 12. Cases of SST failure modes: (a) WC, (b) BI, and (c) WC-BI.

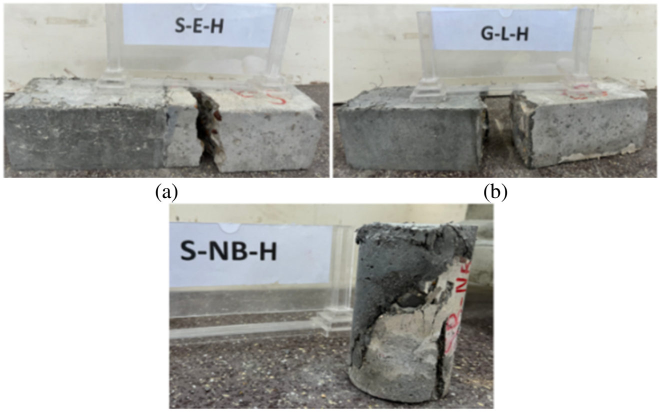

(a) (b)

(c)

Fig. 13. Cases of FBT failure modes: (a) WC, (b) BI, and (c) WC-BI.

This phenomenon can be attributed to the design of the splitting TBT, in which the load is applied in a concentrated line manner on the bond plane surface between the old and new concrete. As depicted in Figure 14, the specimens underwent a splitting tensile bond strength test, with the ACI 546.3R-14 [31] suggesting a range of 14 MPa-21 MPa for the SST. This range signifies the minimum acceptable slant shear bond strength (σ_o) value. Table VI presents the failure modes of the SST and FBS tested samples, as well as the evaluation of the SST samples according to the ACI 546.3R-14. The term "bond strength" is defined as the strength in the context of the BI failure mode, wherein the failure occurs exclusively at the BI. In the other two scenarios, only a lower estimate of the bond strength can be obtained, as long as the failure mechanism relies on the strength of the weaker concrete, in addition to the interfacial bond strength [19, 21]. The majority of the specimens that were examined failed not only due to issues with the bond surface, but also because the failure mechanism was dependent on the WC strength. Consequently, in the majority of the cases examined, the research was unable to ascertain the precise bond strength; instead, it could only estimate the minimum bond strength. However, the results obtained from this study are beneficial because of the comparison of the bonding systems examined and the identification of the most effective surface preparation methods and the most efficient bonding agent.

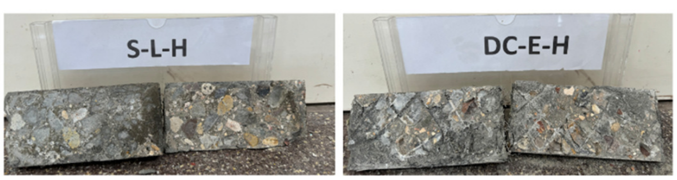

Fig. 14. Cases of TBT.

The magnitude of bond strength exhibited a decrease in the following sequence, as determined by the test method: SST, FBT, and TBT. The findings suggest that the usage of epoxy as a bonding agent, in conjunction with the same surface preparation method, yielded superior bond performance in comparison to latex (synthetic rubber emulsion) across all conducted tests. The samples without a bonding agent demonstrated the poorest performance. The usage of epoxy resin as a bonding agent ensures optimal bond strength, irrespective of the method employed for surface preparation, while on surfaces that underwent G as the sole method of surface preparation, which is the least effective approach among those examined, resulted in a shift in failure mode from BI in the absence of a bonding agent and/or latex bonding agent to the WC failure.

TABLE VI. FAILURE MODES AND EVALUATION OF THE SST AND FBT COMPOSITES

Specimen designation	FBS test	SST	SST sample evaluation according to ACI 546.3R
G-NB-H	BI	BI	Not satisfied
G-E-H	WC	WC	Satisfied
G-L-H	BI	BI	Not satisfied
DC-NB-H	WC-BI	WC-BI	Not satisfied
DC-E-H	WC	WC	Satisfied
DC-L-H	WC	WC	Satisfied
S-NB-H	WC-BI	WC-BI	Not satisfied
S-E-H	WC	WC	Satisfied
S-L-H	WC-BI	WC-BI	Not satisfied
DC-E-W	WC	WC	Satisfied
DC-E-S	WC	WC	Satisfied
DC-E-MH	WC	WC	Satisfied
DC-E-MS	WC	WC	Satisfied

The findings suggest that the surface preparation method exerts a substantial influence on the bond performance. For a given bonding agent, the surface preparation methods employed on the examined specimens, ordered from least to most effective, are G, S, and DC. The findings of this study demonstrate that both DC and S, when used as surface preparation methods without the addition of a bonding agent, effectively eliminated the BI failure mode in both the SST and FBT. The application of both DC and S methods, in the absence of a binder, resulted in a shift from the BI failure to a combination of failure modes in the WC-BI. In the case of the latex binder application on the sample prepared by S, the failure mode remains WC-BI. However, when the latex binder is applied to the bond surface that has been prepared by G and DC, failure occurs in WC. Consequently, it can be deduced that the G and DC surface preparation is more efficacious than the G and S in enhancing the bond performance and increasing the probability of altering the failure mode to failure in the WC. The most effective bond performance among the examined SST, FBT, and TBT bonding systems is yielded by combining the G and DC surface preparation method with the epoxy resin bonding agent. In comparison to the absence of a bonding agent, the usage of epoxy and latex as binders resulted in an enhancement of the bond strength by 108.7% and 17.4%, respectively, when the surface underwent G preparation, 44.7% and 25% when DC was used, and 38.8% and 11.11% for the surfaces subjected to S. The application of an epoxy binder in conjunction with the G surface preparation resulted in a shift in the failure mode from failure at the bond surface to failure within the WC. Consequently, epoxy resulted in a substantial 108.7% increase in the bond strength. When a latex binder is used, the failure mode remains at the bond surface, and the bond strength increase is considerably less than with epoxy. The discrepancy in the contributions of the bond strength between the epoxy and latex diminishes when the DC surface preparation method is adopted, although epoxy continues to demonstrate superior performance. This outcome can be attributed to the use of both epoxy and latex, which led to a shift in the failure mode from failure in both the bond surface and WC to failure exclusively in the WC. In comparison with the surface preparation by G, the usage of S and DC resulted in an increase in the bond strength by 56.5% and 65.2%, respectively, in the absence of a binder. When latex was employed as a binder, the increases were 48.1% and 75.9%, respectively. Using an epoxy bonding agent yielded an increase of 4.2% and 14.6%, respectively, while implementing epoxy-based resin for all surface preparation methods led to a reduction in the impact of the surface preparation strategy on the bond strength. In all cases, failure occurred in the WC, and the measured bond strengths were similar. The findings indicate that the enhancement in bond strength is dependent on both the type of bonding agent and the surface preparation method. In the event of a transition in the failure mode from BI to BI-WC or from BI-WC to WC, as a result of the combined effects of the surface roughening and chemical bonding, an observable increase will be detected. A shift in the failure mode from BI to WC would result in amplified growth. However, if the failure mode remains unchanged, the increase will be negligible.

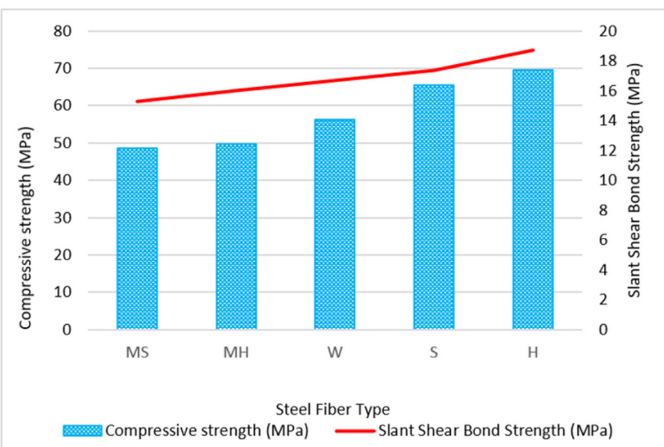

Fig. 15. The relationship between the increasing compressive strength of the SIFCON overlay and the corresponding increase in slant shear bond strength.

The geometry of the steel fiber used had a significant influence on the mechanical properties of the hardened SIFCON overlay. The values of compression, flexural, and tensile strength increased in the following sequence: MS, MH, W, S, and H. The increase in the compressive strength of the overlay had a significant effect on the SST results. As shown in Figure 15, there is a direct correlation between the enhancement of compressive strength exhibited by the SIFCON overlay and the concomitant increase in slant shear bond strength. The slant shear bond strength exhibited an increase with the rise in the overlay's compressive strength. Conversely, the FBT and TBT results showed minimal sensitivity to the variations in compressive strength. The findings of this study indicate a direct proportional relationship between the compression ratio of the overlay to the substrate and the slant shear bond strength.

V. CONCLUSIONS

The following conclusions can be drawn from this study:

- The evaluation of the bond strength demonstrated a substantial dependence on the employed method of testing. The magnitude of the bond strength exhibited a decrease in the following sequence, as determined by the test method: Slant Shear Test (SST), Flexural Bond Test (FBT), and Tensile Bond Test (TBT).
- Despite the inability of the study to ascertain the true bond strength, owing to the failure mechanism's reliance on Weaker Concrete (WC) strength, it was able to evaluate only the minimum estimated bond strength in the majority of the specimens examined. Nevertheless, the results obtained from this study enabled a comparative analysis of the examined bonding systems and facilitated the identification of the most effective surface preparation methods and the optimal bonding agent.
- In the course of the experiments conducted, epoxy was used as a bonding agent, resulting in superior bond performance in comparison to the sample counterparts that lacked a binder or those that employed latex.
- A comparison of the results obtained with and without the use of a bonding agent reveals that the incorporation of epoxy and latex as binders resulted in a 108.7% and 17.4% increase in the bond strength, respectively, when the surface was prepared by Grinding (G). This increase was observed to be 44.7% and 25% when Diamond Cutting (DC) was employed, and 38.8% and 11.11% for surfaces that underwent Sandblasting (S).
- The method of surface preparation exerted a substantial influence on the performance of the bonds. For the same bonding agent, the surface preparation methods employed on the examined specimens, ranked in ascending order, are G, S, and DC.
- A comparative analysis was conducted to assess the impact of different surface preparation methods on the bond strength of the materials. The experiment included G, S, and DC as surface preparation techniques. The results showed that the use of S and DC methods resulted in a significant increase in the bond strength, with an increase of 56.5% and 65.2%, respectively, when no binder was used. When latex was used as a binder, the bond strength increased by 48.1% and 75.9%, respectively. Finally, the use of an epoxy bonding agent resulted in an increase of 4.2% and 14.6%, respectively.
- The usage of epoxy-based resin for all surface preparation methodologies resulted in a reduction of the impact of the surface preparation strategy on the bond strength. In all cases, failure occurred in the weaker concrete, and the measured bond strengths were similar.

- The enhancement in bond strength is influenced by two factors: the type of bonding agent used and the method of surface preparation. When the combined effects of the surface roughening and chemical bonding cause a change in the failure mode from the Bond Interface (BI) to failure in both BI and Weaker Concrete (BI-WC) or from BI-WC to WC, the increase will be noticeable. If the failure mode shifts directly from BI to WC, the growth will be even more significant. However, if the failure mode remains unchanged, the increase will be negligible.
- The geometry of the steel fibers used had a substantial impact on the mechanical properties of the hardened SIFCON overlay, thereby exerting a notable influence on the SST outcomes. The slant shear bond strength exhibited an increase with the rise in the overlay's compressive strength. Conversely, the FBT and TBT results demonstrated no significant alteration. A direct proportional relationship between the compression ratio of the overlay and the substrate, and the slant shear bond strength, has been observed.

In this study, due to the limited sample size and the constraints outlined by ACI 546.3R-14 [31], a comparative analysis of the chipping surface preparation method with other methods explored was not conducted. Furthermore, the study did not evaluate the effect of adding dowels on enhancing the bonding performance between the old and new layers. Therefore, a study that assesses the bonding performance through direct shear testing of RC beam sections strengthened with SIFCON jackets can serve as a complementary approach to the current research and a valuable suggestion for future work.

REFERENCES

[1] R. A. Barnes, P. S. Baglin, G. C. Mays, and N. K. Subedi, "External steel plate systems for the shear strengthening of reinforced concrete beams," *Engineering Structures*, vol. 23, no. 9, pp. 1162–1176, Sept. 2001, https://doi.org/10.1016/S0141-0296(00)00124-3.

[2] A. Abu-Obeidah, R. A. Hawileh, and J. A. Abdalla, "Finite element analysis of strengthened RC beams in shear with aluminum plates," *Computers & Structures*, vol. 147, pp. 36–46, Jan. 2015, https://doi.org/10.1016/j.compstruc.2014.10.009.

[3] M. Ipek and M. Aksu, "The effect of different types of fiber on flexure strength and fracture toughness in SIFCON," *Construction and Building Materials*, vol. 214, pp. 207–218, July 2019, https://doi.org/10.1016/j.conbuildmat.2019.04.055.

[4] M. Ipek, M. Aksu, K. Yilmaz, and M. Uysal, "The effect of pre-setting pressure on the flexural strength and fracture toughness of SIFCON during the setting phase," *Construction and Building Materials*, vol. 66, pp. 515–521, Sept. 2014, https://doi.org/10.1016/j.conbuildmat.2014.04.107.

[5] A. M. Abbas, H. K. Hussain, and M. F. Ojaimi, "Shear and Flexural Behavior of Flat Slabs Casted with Polyolefin Fiber-Reinforced Concrete," *Fibers*, vol. 10, no. 4, Apr. 2022, Art. no. 34, https://doi.org/10.3390/fib10040034.

[6] M. F. Ojaimi, M. K. Eb. Altaee, and N. S. Aljabbri, "Structural behavior of two-way slabs cast with different fiber types and contents," *Periodicals of Engineering and Natural Sciences (PEN)*, vol. 9, no. 3, Sept. 2021, Art. no. 831, https://doi.org/10.21533/pen.v9i3.2314.

[7] A. Mohan, S. Karthika, J. Ajith, L. dhal, and M. Tholkapiyan, "Investigation on ultra high strength slurry infiltrated multiscale fibre reinforced concrete," *Materials Today: Proceedings*, vol. 22, pp. 904–911, Jan. 2020, https://doi.org/10.1016/j.matpr.2019.11.102.

[8] A. A. Manolia, A. S. Shakir, and J. F. Qais, "The effect of fiber and mortar type on the freezing and thawing resistance of Slurry Infiltrated Fiber Concrete (SIFCON)," *IOP Conference Series: Materials Science and Engineering*, vol. 454, no. 1, Sept. 2018, Art. no. 012142, https://doi.org/10.1088/1757-899X/454/1/012142.

[9] S. S. Khamees, M. M. Kadhum, and N. A. Alwash, "Effects of Steel Fibers Geometry on the Mechanical Properties of SIFCON Concrete," *Civil Engineering Journal*, vol. 6, no. 1, pp. 21–33, Jan. 2020, https://doi.org/10.28991/cej-2020-03091450.

[10] O. Sengul, "Mechanical properties of slurry infiltrated fiber concrete produced with waste steel fibers," *Construction and Building Materials*, vol. 186, pp. 1082–1091, Oct. 2018, https://doi.org/10.1016/j.conbuildmat.2018.08.042.

[11] S. G. Gok and O. Sengul, "Enhancing Mechanical Properties of Alkali-Activated Slag SIFCON for Sustainable Construction Using Recycled Glass and Tire-Derived Waste Steel Fibers," *International Journal of Concrete Structures and Materials*, vol. 18, no. 1, Dec. 2024, Art. no. 89, https://doi.org/10.1186/s40069-024-00724-6.

[12] S. G. Gok and O. Sengul, "Mechanical properties of alkali-activated slag based SIFCON incorporating waste steel fibers and waste glass," *Construction and Building Materials*, vol. 408, Dec. 2023, Art. no. 133697, https://doi.org/10.1016/j.conbuildmat.2023.133697.

[13] T. E. Ibrahim, O. A. Abdulrazzaq, and S. M. Saleh, "Bonding between New and Old Concrete in Composite Beams under the Effect of Static Loads," *Engineering, Technology & Applied Science Research*, vol. 14, no. 5, pp. 16646–16652, Oct. 2024, https://doi.org/10.48084/etasr.8323.

[14] T. E. Ibrahim, O. A. Abdulrazzaq, and S. M. Saleh, "Bonding between New and Substrate Concrete in Composite Beams subjected to the Effect of Repeated Loads," *Engineering, Technology & Applied Science Research*, vol. 14, no. 5, pp. 17149–17155, Oct. 2024, https://doi.org/10.48084/etasr.8392.

[15] E. N. B. S. Júlio, F. A. B. Branco, and V. D. Silva, "Concrete-to-concrete bond strength. Influence of the roughness of the substrate surface," *Construction and Building Materials*, vol. 18, no. 9, pp. 675–681, Nov. 2004, https://doi.org/10.1016/j.conbuildmat.2004.04.023.

[16] K. Behfarnia, H. Jon-nesari, and A. Mosharaf, "The bond between repair materials and concrete substrate in marine environment," *Asian Journal of Civil Engineering (Building and Housing)*, vol. 6, no. 4, pp. 267–272, 2005.

[17] Z. Wan, "Interfacial shear bond strength between old and new concrete," M.S. thesis, Louisiana State University and Agricultural and Mechanical College, Baton Rouge, LA, USA, 2010.

[18] T. E. Ibrahim, O. A. Abdulrazzaq, and S. M. Saleh, "Slant Shear Bonding Between Old and New Concrete," in *Current Trends in Civil Engineering and Engineering Sciences 2024, Vol 2*, Singapore, 2025, pp. 382–396, https://doi.org/10.1007/978-981-97-9368-6_28.

[19] P. W. Ariyadasa, A. C. Manalo, W. Lokuge, V. Aravinthan, K. Pasupathy, and A. Gerdes, "Bond performance of fly ash-based geopolymer mortar in simulated concrete sewer substrate," *Construction and Building Materials*, vol. 446, Oct. 2024, Art. no. 137927, https://doi.org/10.1016/j.conbuildmat.2024.137927.

[20] A. M. Diab, A. E. M. Abd Elmoaty, and M. R. Tag Eldin, "Slant shear bond strength between self compacting concrete and old concrete," *Construction and Building Materials*, vol. 130, pp. 73–82, Jan. 2017, https://doi.org/10.1016/j.conbuildmat.2016.11.023.

[21] R. Saldanha, E. Júlio, D. Dias-da-Costa, and P. Santos, "A modified slant shear test designed to enforce adhesive failure," *Construction and Building Materials*, vol. 41, pp. 673–680, Apr. 2013, https://doi.org/10.1016/j.conbuildmat.2012.12.053.

[22] *C150/C150M-24 Standard Specification for Portland Cement*. West Conshohocken, PA, USA: ASTM International, 2024.

[23] *C1240-20 Standard Specification for Silica Fume Used in Cementitious Mixtures*. West Conshohocken, PA, USA: ASTM International, 2020.

[24] *C33/C33M-18 Standard Specification for Concrete Aggregates*. West Conshohocken, PA, USA: ASTM International, 2018.

[25] *C494/C494M-10a Standard Specification for Chemical Admixtures for Concrete*. West Conshohocken, PA, USA: ASTM International, 2017.

[26] *C496/C496M-17 Standard Test Method for Splitting Tensile Strength of Cylindrical Concrete Specimens*. West Conshohocken, PA, USA: ASTM International, 2017.

[27] *C78/C78M-22 Standard Test Method for Flexural Strength of Concrete (Using Simple Beam with Third-Point Loading)*. West Conshohocken, PA, USA: ASTM International, 2018.

[28] *C1437-20 Standard Test Method for Flow of Hydraulic Cement Mortar*. West Conshohocken, PA, USA: ASTM International, 2020.

[29] *The European Guidelines for Self-Compacting Concrete: Specification, Production and Use*. Flums, Switzerland: EFNARC, 2005.

[30] H. Yazıcı, S. Aydın, H. Yiğiter, M. Y. Yardımcı, and G. Alptuna, "Improvement on SIFCON Performance by Fiber Orientation and High-Volume Mineral Admixtures," *Journal of Materials in Civil Engineering*, vol. 22, no. 11, pp. 1093–1101, Nov. 2010, https://doi.org/10.1061/(ASCE)MT.1943-5533.0000114.

[31] *PRC-546.3-14 Guide to Materials Selection for Concrete Repair*. Farmington Hills, MI, USA: ACI, 2014.

[32] *C882/C882M-20 Standard Test Method for Bond Strength of Epoxy-Resin Systems Used With Concrete By Slant Shear*. West Conshohocken, PA, USA: ASTM International, 2020.

[33] J. Kreigh, "Arizona slant shear test: a method to determine epoxy bond strength," *ACI Journal*, vol. 73, no. 7, pp. 372–373, 1976.

[34] S. Austin, P. Robins, and Y. Pan, "Shear bond testing of concrete repairs," *Cement and Concrete Research*, vol. 29, no. 7, pp. 1067–1076, July 1999, https://doi.org/10.1016/S0008-8846(99)00088-5.

[35] D. Daneshvar, A. Behnood, and A. Robisson, "Interfacial bond in concrete-to-concrete composites: A review," *Construction and Building Materials*, vol. 359, Dec. 2022, Art. no. 129195, https://doi.org/10.1016/j.conbuildmat.2022.129195.

[36] A. A. Bahraq, M. A. Al-Osta, S. Ahmad, M. M. Al-Zahrani, S. O. Al-Dulaijan, and M. K. Rahman, "Experimental and Numerical Investigation of Shear Behavior of RC Beams Strengthened by Ultra-High Performance Concrete," *International Journal of Concrete Structures and Materials*, vol. 13, no. 1, Jan. 2019, Art. no. 6, https://doi.org/10.1186/s40069-018-0330-z.

[37] A. Oktavia, A. Y. Pratiwi, and N. Chairunnisa, "Performance Of Concrete-To-Concrete Bond Strength in Wetland Area," *E3S Web of Conferences*, vol. 476, 2024, Art. no. 01062, https://doi.org/10.1051/e3sconf/202447601062.